

# Influence study of the plasma dynamic method energy parameters on the phase composition of the Al-Mg-O system products

A A Sivkov, A S Ivashutenko, I A Rakhmatullin, Yu L Shanenkova  
and A I Tsimmerman

National Research Tomsk Polytechnic University, 30 Lenin Ave., Tomsk, 634050,  
Russia

E-mail: [sivkovAA@mail.ru](mailto:sivkovAA@mail.ru)

**Abstract.** This article shows the possibility of obtaining aluminum-magnesium-oxygen system materials by plasma dynamic synthesis. The results of the influence study of the coaxial magnetoplasma accelerator input energy on the phase composition of the plasma dynamic synthesis product are presented. X-ray structural analysis showed the possibility of obtaining nanostructured material with the content of the phases of gamma aluminum oxide and some spinels of different stoichiometry. It was found that with increasing the value of the accelerator input energy, the total percentage of the spinel phases decreases from 12 to 7%. The results of transmission electron microscopy confirmed the absence of the spinel phase  $\text{MgAl}_2\text{O}_4$  in the product of plasma dynamic synthesis obtained at a higher value of the input energy.

## 1. Introduction

Nanosized aluminum oxide has excellent properties, such as high radiation sensitivity, hardness and compressive strength or flexural strength, good dielectric characteristics and low density. Such a wide range of characteristics determines its wide application in various fields of science, technology and medicine. [1–2].

Currently, nanostructured materials of the aluminum-oxygen (Al-O) system are produced by the method of electrical explosion of conductors [3], gas-phase [2], sol-gel [4] or laser [5] methods. Each of these methods has its advantages and disadvantages. The main disadvantages are the complexity of the process and its multi-stage.

In this work, the possibility of obtaining nanosized aluminum oxide by the plasma dynamic method. The main element of this method is an erosion-type coaxial magnetoplasma accelerator. A detailed description of the device and the principle of operation of a coaxial magnetoplasma accelerator is presented in articles [6–7]. The method of plasma-dynamic synthesis does not have the above disadvantages. Its main advantages are the simplicity of obtaining the material and the single-stage nature of the synthesis process [8–12].

## 2. Experimental part

The plasma dynamic method is based on the production of aluminum by electroerosion from the cylindrical surface of the acceleration channel. The eroded mass from the accelerator barrel is captured



by the plasma structure of an accelerated high-current discharge under high temperature conditions (about  $10^4$  K). Eroded material enters the plasma state and is carried from the acceleration channel at a speed of about  $10^3$  m·s<sup>-1</sup> into the sealed volume of the chamber-reactor. Previously, the volume of the chamber-reactor is filled with a gaseous precursor – oxygen and argon in a ratio of 4:1 (80% and 20%, respectively).

Plasma chemical synthesis of materials takes place in the chamber-reactor. The synthesized material is sprayed in the liquid phase at the front of the head shock wave of an electric-discharge plasma jet. Further, the crystallization of the powder occurs with the formation of highly dispersed particles of various modifications crystalline phases. The chamber-reactor opening and the synthesized product collection is carried out with the complete precipitation of particles one hour after the process. In one short operation cycle of a coaxial magnetoplasma accelerator (cycle time of about 1 ms), the plasma dynamic method provides for the synthesis of a nanodispersed material based on aluminum-oxygen weighing up to 10 grams. The magnitude of the energy input  $W$ , the duration of the power supply pulse, the parameters of the medium in the chamber-reactor (Ar:O<sub>2</sub> ratio) and other structural and energy parameters of the accelerator system affect the mass of the obtaining material, the phase and morphological composition of the synthesized product [9]. In the work, a comparative analysis of materials obtained by the plasma dynamic method is performed depending on the magnitude of the accelerator energy input  $W$ .

Experiments on the production of nanostructured materials in the aluminum-oxygen system were carried out with the following parameters of a capacitive energy storage: charging voltage  $U_{ch} = 2.1$  kV at capacitance  $C = 14.4$  mF. A series of experiments with a changing the energy supplied to the accelerator was carried out to assess the effect of the input energy  $W(t)$  on the weight of the product, its phase composition and dispersibility. Figure 1 shows the oscillograms of the voltage on the electrodes of the accelerator  $U(t)$  and the discharge current  $I(t)$ , obtained during the experiments. The voltage and current curves were used to construct the discharge power curve  $P(t) = U(t) \cdot I(t)$ . Integration of the discharge power curve allows us to estimate the amount of energy input  $W(i)$ . From the curves  $W(t)$  it can be seen that the value of the input energy varies and is  $W_1 = 19.27$  kJ (a),  $W_2 = 21.14$  kJ (b) and  $W_3 = 22.80$  kJ (c). From the oscillograms one can see that the duration of the process with these parameters is about  $t = 400$   $\mu$ s.

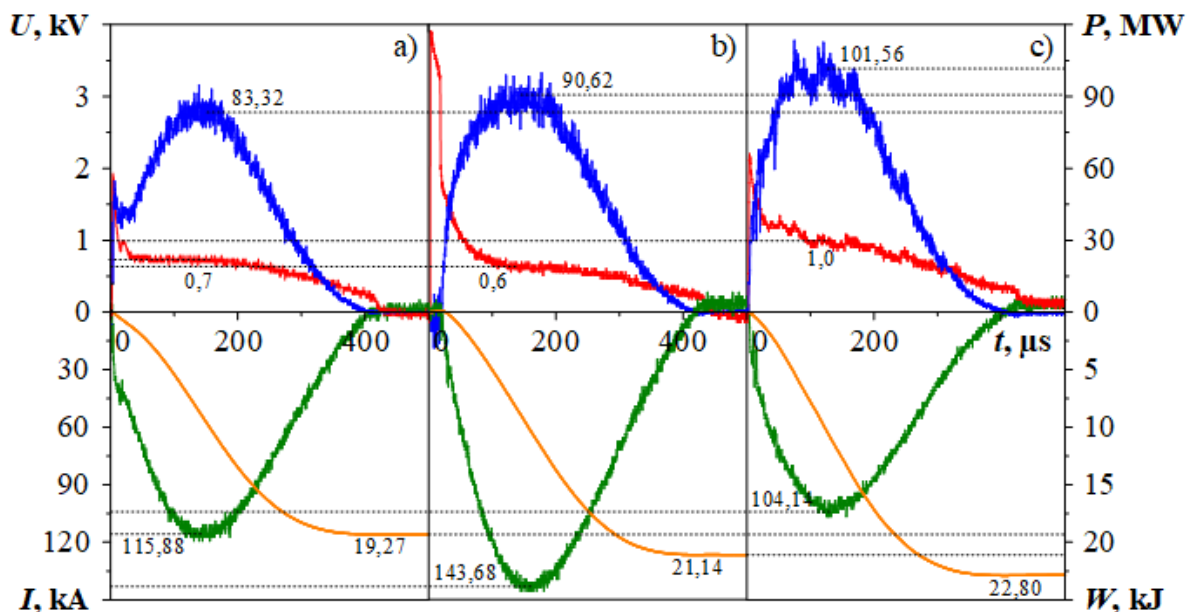


**Figure 1.** Typical oscillograms of the discharged current  $I(t)$ , voltage at the accelerator electrodes  $U(t)$ , curves of the discharge power in the accelerating channel  $P(t)$  and the input energy  $W$  a)  $W_1 = 19.27$  kJ, b)  $W_2 = 21.14$  kJ and c)  $W_3 = 22.80$  kJ.

The product of plasma dynamic synthesis without any preliminary preparations was studied on a Shimadzu XRD 7000S X-ray diffractometer (CuK $\alpha$  radiation) with a Shimadzu CM 3121 monochromator, the results of X-ray phase analysis from which were processed in the Crystallographica Search-Match program. Transmission electron microscopy was performed on a Philips SM 12 microscope in order to analyze the structure and size of the resulting plasma-dynamic synthesis material with an accelerating voltage of 100 kV.

### 3. Results and discussion

To determine the phase composition of the synthesized powders, an X-ray diffraction analysis method was used. Figure 2 shows the XRD patterns of powders obtained at different energy input. The analysis of the obtained diffractions showed the proximity of the synthesized powders to the structural models of gamma aluminum oxygen  $\gamma$ -Al<sub>2</sub>O<sub>3</sub> (card number 50-741, cubic syngony, lattice parameters  $a = b = c = 7.939$  Å) and magnesium spinels Mg<sub>0.4</sub>Al<sub>2.4</sub>O<sub>4</sub> (number cards 87-341, cubic syngony, lattice parameters  $a = b = c = 7.9543$  Å), MgAl<sub>26</sub>O<sub>40</sub> (card number 20-660, tetragonal syngony, lattice parameters  $a = b = 7.956$  Å,  $c = 11.745$  Å) and MgAl<sub>2</sub>O<sub>4</sub> (card number 75-1800, cubic syngony, lattice parameters  $a = b = c = 8.1311$  Å).

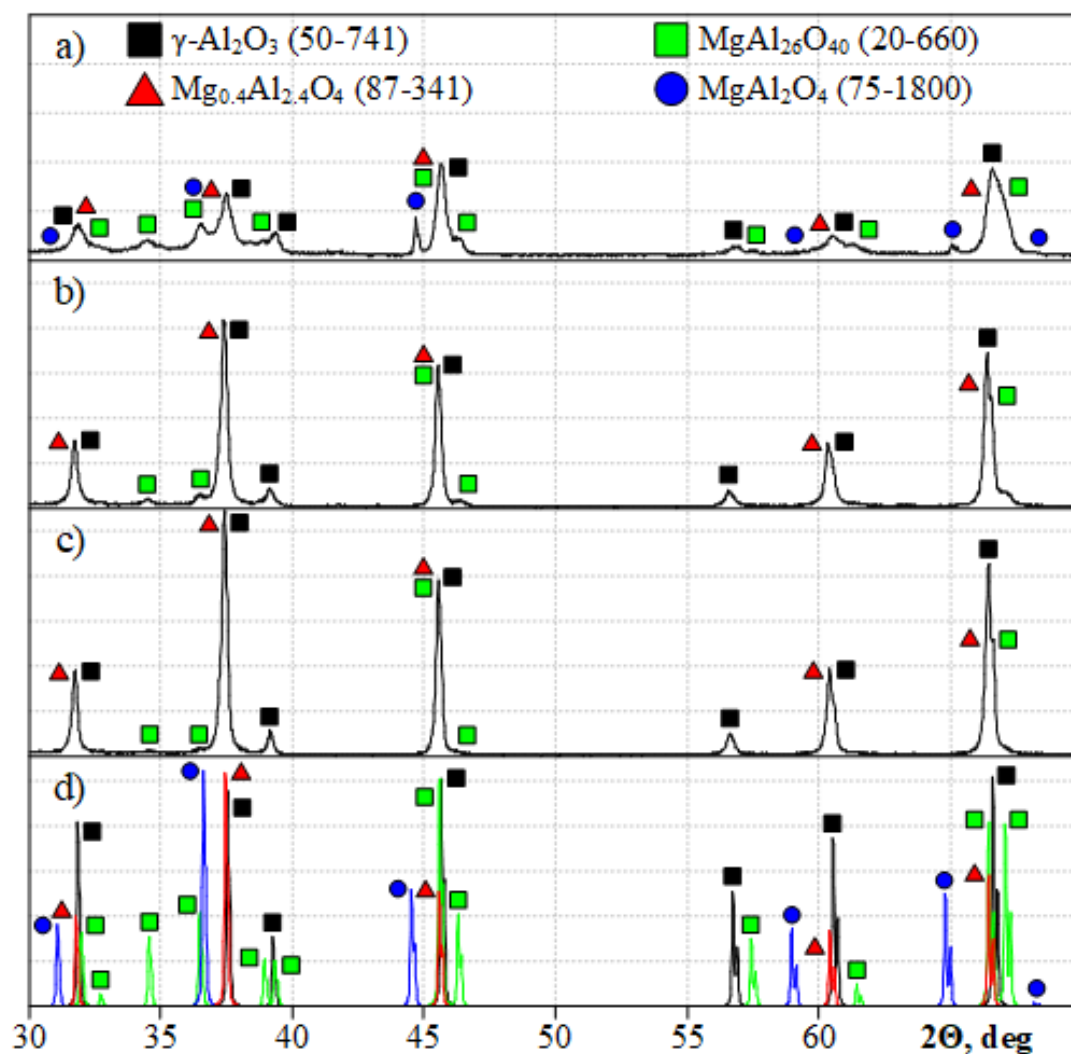


**Figure 2.** Diffractograms of the obtained plasmodynamic synthesis powdery products: a)  $W_1 = 19.27$  kJ, b)  $W_2 = 21.14$  kJ, c)  $W_3 = 22.80$  kJ and d) Material cards from the PDF4 + database.

The presence of magnesium spinel is explained by the fact that 7% of magnesium is present in the composition of the barrel used in the experiments. It is known that the addition of the magnesium spinel group makes it possible to improve the properties of aluminum oxide [13]; therefore, this manifestation factor of magnesium spinel in the products of plasma dynamic synthesis will not adversely affect the characteristics of the product.

It should be noted that magnesium spinel with  $\text{MgAl}_2\text{O}_4$  stoichiometry is present only in the material obtained at the lowest accelerator energy input (figures 1–2(a)). While increasing the value to  $W_2 = 21.14$  kJ, the intensity of this phase becomes zero and even at the level of traces, figures 1–2(b) is not identified in the products of plasma dynamic synthesis. At the same time, against the background of an increase in the input energy  $W$ , the intensity of the  $\text{MgAl}_{26}\text{O}_{40}$  phase decreases, and the phases of aluminum oxide  $\gamma\text{-Al}_2\text{O}_3$  and magnesium spinel with  $\text{Mg}_{0.4}\text{Al}_{2.4}\text{O}_4$  stoichiometry become dominant in the product obtained in experiments (b and c). The percentage of the aluminum oxide phase increases with an increase in the input energy of the accelerator from 87.4% to 92.7%, while the phases of magnesium spinel decrease from 12.6% to 7.3%.

A comparative analysis of X-ray diffraction patterns of products obtained at different energies, allows us to conclude that with increasing energy, the intensities of the  $\gamma\text{-Al}_2\text{O}_3$  and phases  $\text{Mg}_{0.4}\text{Al}_{2.4}\text{O}_4$  increase. Thus, depending on the objectives, it is possible to control the phase composition of the product of the plasma dynamic synthesis of the aluminum-magnesium-oxygen system.

The results of transmission electron microscopy of plasma dynamic synthesis products obtained at the lowest  $W_1 = 19.27$  kJ (figures 1–2(a)) and the highest  $W_3 = 22.80$  kJ (figures 1–2(c)) of the input energy of the coaxial magnetoplasma accelerator are presented in figure 3.

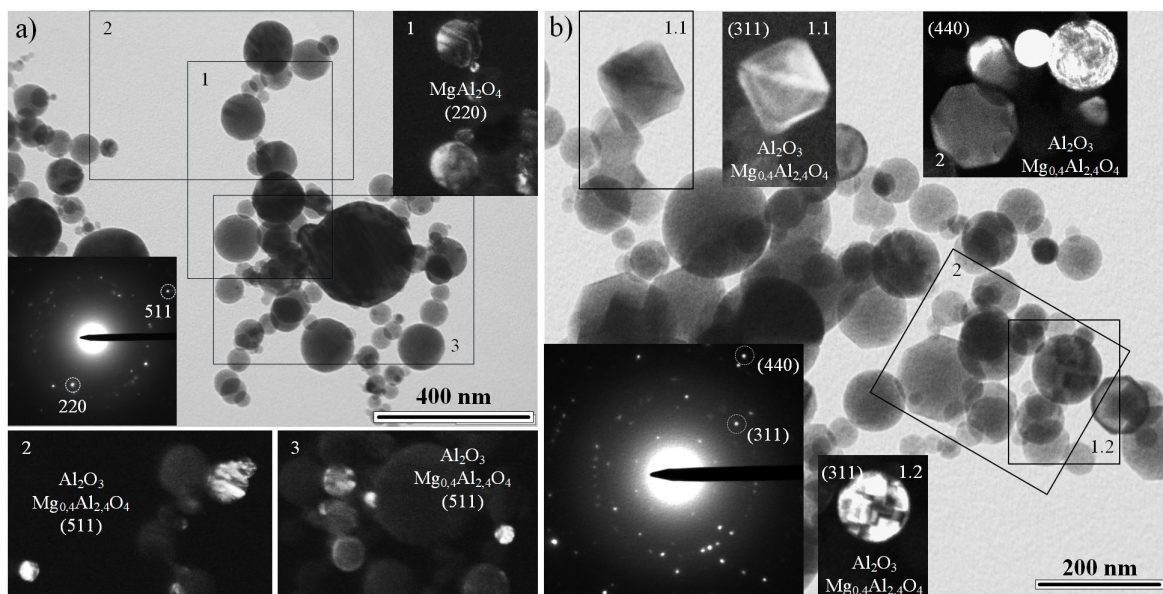


**Figure 3.** TEM-images of synthesized materials a)  $W_1 = 19.27$  kJ and b)  $W_3 = 22.80$  kJ.

From the light-field and dark-field TEM images of the accumulation of particles of synthesized materials, it can be seen that with a relatively low energy input  $W_1 = 19.27$  kJ (under the conditions considered) almost all particles have a rounded shape. With increasing energy up to  $W_3 = 22.80$  kJ, one can observe an increase in the material in size and the acquisition of some particles of more stringent geometric forms. Such a difference in the shape of particles obtained under different energy conditions can be explained by a higher temperature of the synthesis process at a high level of energy input and, as a result, the shape of the particles becomes more even. So, for example, in a dark-field TEM image (figure 3b(1.1)), an almost perfectly square is clearly visible, which can be identified

using electron microdiffraction as  $\gamma$ -Al<sub>2</sub>O<sub>3</sub> aluminum oxide gamma phase in the [311] direction and magnesium spinel phase Mg<sub>0.4</sub>Al<sub>2.4</sub>O<sub>4</sub> [311]. Light-field and dark-field pictures of reflex 2 on the same SAED (figure 3b(2)) are also characterized by the presence of particles of a more regular geometric cut, resembling octagons, and are determined, as in the previous case, by the same phases in the [440] direction.

The results of transmission electron microscopy unambiguously confirm the fact of the presence of the MgAl<sub>2</sub>O<sub>4</sub> spinel phase in the product obtained with a smaller amount of input energy (figures 1–3(a)), and the absence of this phase in the material synthesized already at  $W_3 = 22.80$  kJ (figures 1–2(c), 3b).

#### 4. Conclusion

Thus, the paper shows the possibility of obtaining a highly dispersed single-crystal powder of aluminum oxide using the plasma dynamic method using a system based on a coaxial magnetoplasma accelerator with an aluminum accelerating channel. During the study of the effect of the input energy  $W$  on the phase composition of the synthesized powder system Al-Mg-O, that an increase in  $W$  in the range from 19 to 23 kJ is accompanied by a change in the phase composition. It was revealed that with increasing  $W$ , the content of Al-Mg-O phases of  $\gamma$ -Al<sub>2</sub>O<sub>3</sub> and Mg<sub>0.4</sub>Al<sub>2.4</sub>O<sub>4</sub> in the system increases, the MgAl<sub>26</sub>O<sub>40</sub> phase decreases, and the MgAl<sub>2</sub>O<sub>4</sub> phase is not detected. It should be noted that the percentage of gamma-phase aluminum oxide increases with an increase in the input energy of the accelerator from 87.4% to 92.7%, while the sum mass phases of magnesium spinels decrease from 12.6% to 7.3%.

#### References

- [1] Vorozhtsov A B, Lerner M., Rodkevich N, Nie H, Abraham A, Schoenitz M and Dreizin E L 2016 *Thermochim. Acta.* **636** 48
- [2] Kortov V S, Ermakov A E, Zatsepin A F, Uymin M A, Nikiforov S V, Mysik A A and Gaviko V S 2008 *Fizika tverdogo tela* **50** 916
- [3] Kotov Yu A and Ivanov V V *Vestnik Rossijskoj akademii nauk* **78** 777
- [4] Brinker C J and Scherer G W 2013 *Academic press*
- [5] Svetlichnyy V A, Stadnichenko A I and Lapin I N 2017 *Izvestiya vysshikh uchebnykh zavedeniy. Fizika* **60** 157
- [6] Shanenkov I, Sivkov A, Ivashutenko A, Medvedeva T and Shchetinin I 2019 *J. Alloys Compd.* **774** 637
- [7] Sivkov A, Ivashutenko A, Shanenkova Y, Shanenkov I, Rakhmatullin I and Osokina L 2018 *Ceram. Int.* **44** 22808
- [8] Kuzenov V V, Polozova T N and Ryzhkov S V 2015 *Probl. Atomic Science Technology* **4** 49
- [9] Sivkov A A, Ivashutenko A S, Rakhmatullin I A, Shanenkova Y L and Tsimmerman A I 2018 *Nanotechnologies in Russia* **13** 76
- [10] Sivkov A A, Pak A Y, Nikitin D S, Rakhmatullin I A and Shanenkov I I 2013 *Nanotechnologies in Russia* **8** 489
- [11] Shanenkov I I, Pak A Y, Sivkov A A and Shanenkova Y L 2014 *MATEC Web Conf.* **19** 01030
- [12] Sivkov A, Saygash A, Kolganova J and Shanenkov I 2014 *IOP Conference Series: Mater. Sci. Eng.* **66** 012048
- [13] Braulio M A L, Rigaud M, Buhr A, Parr C and Pandolfelli V C 2011 *Ceramics International* **37** 1705